



Communication

Aptamer-Sensitized Nanoribbon Biosensor for Ovarian Cancer Marker Detection in Plasma

Yuri D. Ivanov ^{1,2,*}, Kristina A. Malsagova ¹ , Tatyana O. Pleshakova ¹, Rafael A. Galiullin ¹, Andrey F. Kozlov ¹, Ivan D. Shumov ¹, Vladimir P. Popov ³ , Svetlana I. Kapustina ¹, Irina A. Ivanova ¹, Arina I. Isaeva ¹, Fedor V. Tikhonenko ³, Nikolay E. Kushlinskii ⁴, Alexander A. Alferov ⁴, Vadim Yu. Tatur ⁵, Vadim S. Ziborov ^{1,2}, Oleg F. Petrov ², Alexander V. Glukhov ⁶ and Alexander I. Archakov ¹

¹ Institute of Biomedical Chemistry, 119121 Moscow, Russia; kristina.malsagova86@gmail.com (K.A.M.); t.pleshakova1@gmail.com (T.O.P.); rafael.anvarovich@gmail.com (R.A.G.); afkozlow@mail.ru (A.F.K.); shum230988@mail.ru (I.D.S.); sveta.kapustina7.05@gmail.com (S.I.K.); i.a.ivanova@bk.ru (I.A.I.); arina.atom@gmail.com (A.I.I.); ziborov.vs@yandex.ru (V.S.Z.); alexander.archakov@ibmc.msk.ru (A.I.A.)

² Joint Institute for High Temperatures of Russian Academy of Sciences, 125412 Moscow, Russia; ofpetrov@ihed.ras.ru

³ Rzhanov Institute of Semiconductor Physics, Siberian Branch of Russian Academy of Sciences, 630090 Novosibirsk, Russia; popov@isp.nsc.ru (V.P.P.); ftikhonenko@gmail.com (F.V.T.)

⁴ N.N. Blokhin National Medical Research Center of Oncology, 115478 Moscow, Russia; kne3108@gmail.com (N.E.K.); biochimia@yandex.ru (A.A.A.)

⁵ Foundation of Perspective Technologies and Novations, 115682 Moscow, Russia; v_tatur@mail.ru

⁶ JSC Novosibirsk Plant of Semiconductor Devices with OKB, 630082 Novosibirsk, Russia; gluhov@nzpp.ru

* Correspondence: yurii.ivanov.nata@gmail.com; Tel.: +7-499-246-3761



Citation: Ivanov, Y.D.; Malsagova, K.A.; Pleshakova, T.O.; Galiullin, R.A.; Kozlov, A.F.; Shumov, I.D.; Popov, V.P.; Kapustina, S.I.; Ivanova, I.A.; Isaeva, A.I.; et al. Aptamer-Sensitized Nanoribbon Biosensor for Ovarian Cancer Marker Detection in Plasma. *Chemosensors* **2021**, *9*, 222. <https://doi.org/10.3390/chemosensors9080222>

Academic Editor: Dieter Frense

Received: 26 July 2021

Accepted: 9 August 2021

Published: 13 August 2021

Publisher's Note: MDPI stays neutral with regard to jurisdictional claims in published maps and institutional affiliations.



Copyright: © 2021 by the authors. Licensee MDPI, Basel, Switzerland. This article is an open access article distributed under the terms and conditions of the Creative Commons Attribution (CC BY) license (<https://creativecommons.org/licenses/by/4.0/>).

Abstract: The detection of CA 125 protein in buffer solution with a silicon-on-insulator (SOI)-based nanoribbon (NR) biosensor was experimentally demonstrated. In the biosensor, sensor chips, bearing an array of 12 nanoribbons (NRs) with n-type conductance, were employed. In the course of the analysis with the NR biosensor, the target protein was biospecifically captured onto the surface of the NRs, which was sensitized with covalently immobilized aptamers against CA 125. Atomic force microscopy (AFM) and mass spectrometry (MS) were employed in order to confirm the formation of the probe–target complexes on the NR surface. Via AFM and MS, the formation of aptamer–antigen complexes on the surface of SOI substrates with covalently immobilized aptamers against CA 125 was revealed, thus confirming the efficient immobilization of the aptamers onto the SOI surface. The biosensor signal, resulting from the biospecific interaction between CA 125 and the NR-immobilized aptamer probes, was shown to increase with an increase in the target protein concentration. The minimum detectable CA 125 concentration was as low as 1.5×10^{-17} M. Moreover, with the biosensor proposed herein, the detection of CA 125 in the plasma of ovarian cancer patients was demonstrated.

Keywords: ovarian cancer; nanoribbon biosensor; silicon-on-insulator; CA 125; aptamers; surface functionalization

1. Introduction

The effectiveness of cancer therapy depends on the stage at which the disease is revealed; timely revelation of cancer facilitates the treatment and improves its effectiveness [1,2]. This is why early revelation of target cancer-associated biomarkers is required. The blood concentration of the majority of proteins, including the known disease markers, is low ($<10^{-13}$ M) [3]. Particularly, Rissin et al. emphasized that at an early stage of cancer in humans, the blood concentration of cancer-associated marker molecules is at femtomolar (10^{-15} M) levels [1]. At the same time, the sensitivity of methods commonly employed in modern clinical practice—such as enzyme-linked immunosorbent assay (ELISA)-based approaches—is much lower, only allowing the achievement of 10^{-12} M to 10^{-7} M detection limits [1]. Another disadvantage of these methods consists of the use of additional labels (such as enzymatic or fluorescent ones).

Biosensor-based detection represents an approach commonly used for the characterization of intermolecular interactions [4], which is applied for biomarker detection [5]. The use of biosensors with sensor elements of nanometer size—such as nanowires and nanoribbons—opens new horizons in biomedical research. These biosensors allow one to perform direct label-free detection of various targets—such as viral particles [6] and biological macromolecules (proteins [7–13] and nucleic acids [14–19])—in real time, attaining low (<1 fM, i.e., <10⁻¹⁵ M) concentration detection limits [20]. The principle of operation of these biosensors consists of recording a modulation of an electric current, flowing through the sensor elements, in the course of binding of target particles (i.e., macromolecules or viral particles of interest) to their surface. The surface-bound molecules play the role of a virtual gate, while the sensor structure itself represents a field-effect transistor (FET) of nanometer size [21]. Since the sensor elements are characterized by a high surface-to-volume ratio [22], a very high sensitivity of the nanoribbon (NR)-based devices towards the target particles is achieved. In theory, the detection limit of a single target particle per individual sensor element is attainable [14]. For viral particles, the single-particle sensitivity of a nanowire biosensor was experimentally demonstrated by Patolsky et al. [6]. For biological macromolecules, femtomolar and even sub-femtomolar detection limits were attained for nucleic acids [15,23] and for proteins [11,20], respectively. In this way, the data reported in the literature clearly demonstrate that nanoribbon biosensors represent very attractive tools for highly sensitive biomarker detection in both research and clinical practice.

Biological molecules are known to express their function through interactions with other molecules [4]. Hence, in a biosensor device intended for clinical applications, biospecific detection of target molecules should be provided. For this purpose, the surface of the sensor elements is functionalized with molecular probes, which are able to selectively bind the target molecules [24]. Sometimes, the sensor chip represents a surface bearing molecular probes against only one target molecule [25]. For clinical applications, however, multiplexed detection is required in order to provide simultaneous detection of several different biomarkers in one sample [7,26]. In the latter case, the single sensor chip contains an array of multiple sensor elements, and each sensor element is sensitized with molecular probes against one distinct target; this is another advantage of nanowire and nanoribbon biosensors [7,8,26].

For the sensitization of the sensor elements, aptamers [11,13] and antibodies [5,8,12] are commonly employed. The time stability and chemical resistance of antibodies are poor, while their production cost is high. In contrast, aptamers, which represent single-stranded DNA or RNA oligonucleotides capable of biospecific binding with target molecules, are characterized by higher chemical and time stability [27,28] and relatively low production costs, thus being devoid of the disadvantages typical of antibodies.

Ovarian cancer ranks fifth in cancer deaths among women, being the cause of more deaths than any other cancer of the female reproductive system. A woman's risk of getting ovarian cancer during her lifetime is about 1 in 78 [29]. In terms of one-year survival rate, 98% of patients diagnosed at stage I survive their disease—compared with 53.8% of patients diagnosed at stage IV [30]. This clearly indicates why the early diagnosis of ovarian cancer represents an urgent problem in medicine. The discovery of carbohydrate antigen 125 (CA 125) has become a key step on the path towards the non-invasive diagnosis and monitoring of ovarian cancer. CA 125 represents a glycoprotein epitope of a high-molecular-weight mucin [31]. Since CA 125 was suggested as a marker of ovarian cancer in 1983, this protein represents a benchmark for monitoring ovarian cancer patients [32].

Biosensor-based detection of CA 125 has recently been reported in a number of papers. Hence, Szymanska et al. [33] developed a surface plasmon resonance imaging (SPRI) biosensor for the label-free detection of CA 125 in human serum; in this biosensor, polyclonal antibodies against CA 125 were employed as molecular probes; however, no real-time measurements were reported in this paper [33]. Mandal et al. [34] reported the fabrication of an electrochemical (carbon nanotubes)-based biosensor, in which monoclonal antibodies against CA 125 were utilized as molecular probes; the authors, however, per-

formed their experiments at a rather high (560 µg/mL) concentration of CA 125. Attia et al. [35] developed a luminescence-based assay for the detection of CA 125 in serum; in this assay, acridinium-ester-labeled monoclonal antibodies were employed as molecular probes, and fluorescein-labeled monoclonal antibodies were used as secondary antibodies—that is, additional labels were employed. Petrova et al. [36] developed an interesting photonic-crystal-based biosensor for the multiplexed, label-free, real-time detection of CA 125 and two breast cancer markers (human epidermal growth factor receptor 2 and cancer antigen 15-3). Monoclonal antibodies against the target biomarkers were used as probe molecules [36]. It should be emphasized that, in contrast to aptamers, antibodies are quite expensive, while exhibiting poorer chemical and time stability, thus leading to the high cost of the assay.

In the present study, a nanoribbon biosensor (NR biosensor) was employed for the detection of CA 125 in buffer solution. The sensor chip, bearing an array of 12 separate nanoribbons, was fabricated on the basis of “silicon-on-insulator” (SOI) structures of n-type conductance. SOI structures represent precisely engineered multilayer semiconductor/dielectric structures, and the technology of fabrication of nanoribbon sensors, based on these structures, was reported by Naumova et al. [37]; the use of this type of structure in advanced silicon devices is promising. SOI structures are fabricated using a complementary metal–oxide–semiconductor (CMOS)-compatible technology [37]. The latter makes our technology of sensor chip fabrication very convenient, since it allows for production scaling and for integration of the NRs with additional electronic circuitry intended for signal processing [37]. The surface of individual NRs was sensitized with aptamers against CA 125, which were used as molecular probes. Atomic force microscopy (AFM) and mass spectrometry (MS) were employed in order to confirm the efficiency of the technique used for the sensitization of the NRs. Such an approach was shown to be an efficient tool in studying antibody–antigen [38] and aptamer–antigen [39,40] complexes on the surface of solid substrates sensitized with molecular probes. Since immobilized aptamers are barely distinguishable on the AFM substrate surface, the efficiency of the sensitization of the substrate surface with aptamers is estimated after the formation of aptamer–antigen complexes on it [39]. Via AFM and MS, the successful formation of aptamer–antigen complexes on the surface of SOI substrates with covalently immobilized aptamers against CA 125 was revealed. This fact confirms the sufficient efficiency of the NR sensitization technique employed. By using the NR biosensor with aptamer-sensitized sensor elements, successful detection of CA 125 at ultralow concentrations was demonstrated, and the CA 125 concentration detection limit was as low as 20 aM (2×10^{-17} M). This value is an order of magnitude lower than that obtained with the use of antibodies against CA 125 as molecular probes [12]. Successful use of the SOI-based NR sensor chips for the revelation of CA 125 in plasma of ovarian cancer patients was been demonstrated. This indicates that the NR biosensor represents a promising tool for clinical applications.

2. Materials and Methods

2.1. Chemicals

The following chemicals were used in our experiments: 3,3'-dithiobis (sulfosuccinimidyl propionate) (DTSSP crosslinker) (Pierce, Waltham, MA, USA); potassium phosphate monobasic (KH_2PO_4 , Sigma-Aldrich, St. Louis, MO, USA); (3-aminopropyl)triethoxysilane (APTES, Sigma-Aldrich, USA); methanol (CH_3OH , Sigma, St. Louis, MO, USA); hydrofluoric acid (HF; Reakhim, Moscow, Russia); ethanol ($\text{C}_2\text{H}_5\text{OH}$; Reakhim, Russia); acetonitrile (Fischer Scientific, Waltham, MA, USA); isopropanol (Acros Organics, Geel, Belgium); ammonium bicarbonate (Sigma-Aldrich, St. Louis, MO, USA); trifluoroacetic acid (TFA; Sigma-Aldrich, St. Louis, MO, USA); α -cyano-4-hydroxycinnamic acid (HCCA; Sigma-Aldrich, St. Louis, MO, USA); and porcine trypsin (Promega Corp., Madison, WI, USA). ZipTip C18 tips were obtained from Millipore Corporation (Billerica, MA, USA). In all experiments, deionized ultrapure water, obtained via a Simplicity UV system (Millipore, Molsheim, France), was used.

2.2. Protein and Aptamers

Aptamers against CA 125 (Cat. No. ATW0055) and γ -synuclein (Cat. No. ATW0048) were purchased from Base Pair Biotechnologies, Inc. (Pearland, TX, USA) (<https://www.basepairbio.com/> (accessed on 10 July 2021)). Both of the aptamers comprised 70 nucleotides (including primer regions), bearing a C12 linker with an amine group.

Recombinant CA 125 protein (molecular weight 110 kDa; $1 \mu\text{M}$ (10^{-6} M) stock solution in potassium phosphate buffer) was purchased from R&D Systems (Minneapolis, MN, USA).

2.3. Sensor Chip Fabrication

The process of fabrication of the nanoribbon sensor chips, along with their characteristics, is described in detail in our previous paper [12]. Briefly, the sensor chips of n-type conductance were fabricated on the basis of SOI structures using CMOS-compatible technology. The thickness of the cut-off silicon layer and the buried oxide (BOX) layer was 32 nm and 300 nm, respectively. The NR sensor elements were $3 \mu\text{m}$ wide, while their thickness and their length were $t = 32 \text{ nm}$ and $l = 10 \mu\text{m}$, respectively. Figure 1 displays a schematic representation and an optical image of the NR sensor chip, and an AFM image of a single NR sensor element.

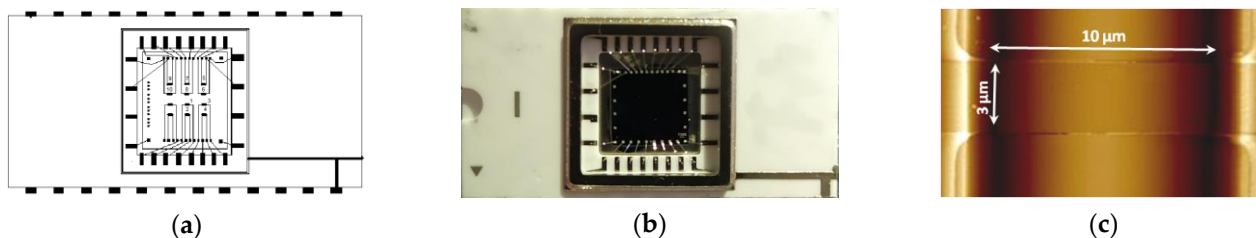


Figure 1. Schematic representation of an NR sensor chip (a); photographic image of an NR chip assembly (b); AFM image of an individual NR sensor. Arrows indicate the dimensions of the sensor (c).

The number of individual NRs on the chip crystal was 12. The NR biosensor setup is described in detail in our previous paper [12].

2.4. Chemical Modification of the Surface of the Nanoribbon Sensor Chip

The surface of the NR sensor chip was treated similarly to the procedure described in our previous paper [12]. Firstly, the chip surface was treated with isopropanol in order to cleanse it of organic contaminants. Secondly, the natural oxide was removed from the clean surface with HF and CH_3OH . The chip was then treated with glow discharge plasma in order to form hydroxyl groups on the sensor surface. After such a treatment, the chip surface was subjected to vapor-phase silanization with APTES [12].

2.5. Covalent Immobilization of Aptamer Molecular Probes onto the NR Surface

The surface of the working NRs was sensitized via covalent immobilization of aptamers against CA 125. In order to account for the non-specific binding, a pair of NRs on the same NR sensor chip was sensitized with aptamers against γ -synuclein (70 nt). The immobilization of the aptamers onto the silanized surface of the individual NRs was carried out in the following manner: Firstly, the APTES-silanized surface of the NR sensor chip was activated with DTSSP crosslinker, as described in our previous papers [11,13]. Secondly, in order to immobilize the aptamers onto the surface of the individual NRs, $\sim 2\text{-nL}$ microdrops of $1\text{-}\mu\text{M}$ solutions of the aptamers in 50-mM potassium phosphate buffer (pH 7.4) were precisely dispensed onto the DTSSP-activated surface of the individual NRs, employing an iONE-600 spotter equipped with a PDMD non-contact microdispenser (M2-Automation, Berlin, Germany; the spotter pertains to the equipment of the “Human Proteome” Core Facility of the Institute of Biomedical Chemistry, supported by Ministry of Education and Science of Russian Federation, Agreement 14.621.21.0017, unique project ID:

RFMEFI62117X0017). Figure 2 displays optical images of the microdroplets of the aptamer solutions dispensed onto the NRs' surface.

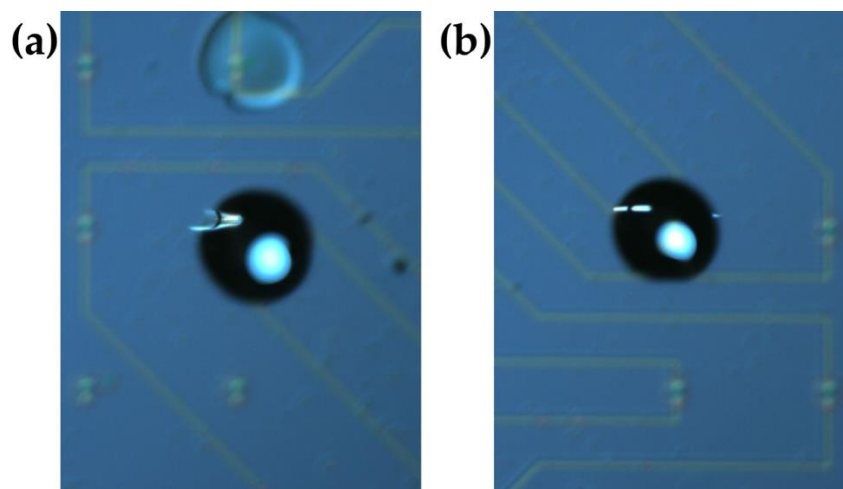


Figure 2. Optical images of the microdroplets of aptamer solutions, dispensed onto the surface of individual 3- μm -wide NRs No. 1, No. 4 (a), and No. 6 (b). The images were obtained via the built-in color CCD camera of the iONE-600 spotter.

The microdroplets were incubated on the NR sensor chip surface for 30 min at 20 °C and 80% RH, before being washed away with ultrapure water and dried in nitrogen flow.

2.6. Preparation of CA 125 Solutions in Buffer

CA 125 solutions with concentrations ranging from 1 aM to 1 fM were prepared from the initial 1- μM stock solution in 50-mM KP buffer (pH 7.4) via sequential tenfold dilution with 1-mM KP buffer (pH 7.4), as described in our previous paper [12], and used in biosensor experiments immediately after preparation.

2.7. AFM Visualization of Aptamer–Target Complexes on the SOI Surface

In order to confirm the efficiency of the sensitization technique developed, atomic force microscopy (AFM) was employed. For this purpose, silicon-on-insulator (SOI) wafers, whose material was identical to that used for the fabrication of the NR sensor chips, were employed as AFM substrates. The procedures of chemical modification and sensitization of the SOI AFM substrates' surface were the same as those used in the case of the NR sensor chips. The SOI AFM substrates with immobilized aptamers against CA 125 were incubated in 10-nM solution of CA 125 in 1-mM KP buffer (pH 7.4). Atomic force microscopy (AFM) images of the surface of the APTES-silanized SOI AFM substrates were obtained using a Dimension FastScan BioTM atomic force microscope (Bruker, Billerica, MA, USA; the microscope pertains to the equipment of the “Human Proteome” Core Facility of the Institute of Biomedical Chemistry, supported by Ministry of Education and Science of Russian Federation, Agreement 14.621.21.0017, unique project ID: RFMEFI62117X0017) in semi-contact mode using ScanAsyst[®] technology. The microscope was equipped with FastScan-B cantilevers (1.8 N/m, tip curvature radius 5 nm). The size of the AFM scans was 2 μm \times 2 μm , the scan resolution was 256 \times 256 points, and the scanning frequency was 1 Hz. In each experiment, no less than 15 scans were obtained, and each experiment was repeated at least three times. The images were recorded using NanoScope 9.4 software (Bruker, Billerica, MA, USA). The treatment of AFM images (flattening correction and digitization for further processing of the AFM data) was performed using standard NanoScope Analysis 1.9 software (Bruker, Billerica, MA, USA). The processing of AFM data was performed using specialized AFM data-processing software developed at the Institute of Biomedical Chemistry.

2.8. Proteolysis on the Surface of SOI Wafers

Trypsinolysis of protein objects, biospecifically captured onto the surface of the aptamer-sensitized SOI AFM substrates, was performed directly in the incubation solution, into which the SOI plates were placed. The incubation solution included 1.75 μL of 0.1- μM modified trypsin in 400- μM (pH 7.4) bicarbonate buffer. After a 20-h incubation, the solution was concentrated using a high-speed vacuum concentrator (5301 Vacufuge Concentrator, Eppendorf, Hamburg, Germany), and then deionized water was added to the solution. The thus-obtained mixture, containing peptide fragments, was desalted using ZipTip C18 tips (Millipore, Temecula, CA, USA) according to the manufacturer's protocol, provided with an Autoflex III time-of-flight (TOF) mass spectrometer [41].

2.9. MALDI-TOF-MS Analysis

Mass spectrometry identification of protein objects, captured onto the linebreakaptamer-functionalized SOI AFM substrates, was performed using an Autoflex III TOF mass spectrometer (Bruker, Karlsruhe, Germany) equipped with a 337-nm N_2 laser. The mass spectrometer was calibrated as described in detail in the previous papers [41,42]. Upon analysis of the mass spectra obtained, peaks resulting from the matrix, along with trypsin autolysis peaks, were excluded. Mass spectrum accumulation was performed in automatic mode until the sample dispensed onto the target was exhausted. Typically, $\sim 10,000$ shots were made.

Processing of the thus-obtained mass spectra was performed using flexAnalysis 2.0 software (Bruker, Karlsruhe, Germany). For the protein identification, the Mascot proteomic search engine (<http://www.matrixscience.com> (accessed on 10 June 2021)) and SwissProt protein sequencing data library were employed [41–43]. The identification was performed by selecting the following search options: (1) taxonomic group: human or eukaryotes; (2) number of missed sites of hydrolysis: two; (3) acceptable measurement accuracy of monoisotopic masses: <150 ppm; (4) possible modification: methionine oxidation. To be considered in the analysis, a mass spectrometric peak should have a signal-to-noise (S/N) ratio of at least two.

2.10. Plasma Samples

The plasma samples studied in our experiments were prepared as follows: Blood samples were obtained either from the patients before treatment, or from the healthy volunteers on an empty stomach. The blood was taken from the cubital vein directly into S-Monovett vacutainers (Sarstedt, Germany) containing 3.8% sodium citrate anticoagulant, and then subjected to a 6-min centrifugation at 3000 rpm (at room temperature). The thus-separated plasma was divided into 500 μL aliquots collected into separate sterile dry test tubes, which were frozen to -70 $^\circ\text{C}$ and stored until their use in the experiments.

Prior to the experiments, each plasma sample was thawed and then diluted 2000-fold with 1-mM potassium phosphate buffer (pH 7.4). The clinical and morphological characteristics of the plasma samples used in the experiments are listed in Table 1.

Table 1. Clinical and morphological characteristics of the plasma samples.

Plasma Sample No.	Age	Sex	Pathology	TNM Stage
1	53	F	Healthy volunteer	–
2	18	F	Healthy volunteer	–
60	67	F	Serous moderate ovarian tumor	T1ANXM0
67	63	F	Serous papillary adenocarcinoma (cyst adenocarcinoma)	T3cNXM1

2.11. Electrical Biosensor Measurements

Electrical measurements with the NR biosensor were performed according to the technique (and using the setup) reported previously [12]. In the experiments on the detection of CA 125 in a purified buffer solution, a 150- μL volume of the CA 125 solution

to be analyzed (in 1-mM KP buffer, pH 7.4) was added to 300 μL of the same pure buffer in the measuring cell. In the experiments on the detection of CA 125 in plasma samples, a 7- μL volume of the plasma sample in 1-mM KP buffer (pH 7.4) was added to 100 μL of pure buffer in the cell. During the biosensor measurements, time dependencies of the drain–source current ($I_{ds}(t)$ dependencies) were recorded at a gate voltage of $V_g = +50$ V, and a drain–source voltage of $V_{ds} = 0.2$ V. In order to account for the non-specific binding of the target protein to the sensor surface, two control NRs, located on the same sensor chip, were sensitized with aptamers against γ -synuclein instead of aptamers against the target CA 125 protein. The signal received from the control NRs was used for the calculation of the differential signal, which was recorded in the form of signal vs. time dependencies and presented graphically in the form of sensogram curves. These curves were recorded in real time, before and after the addition of the analyzed samples to the measuring cell of the biosensor.

3. Results

3.1. Confirmation of the Formation of Probe–Target Complexes on the SOI Surface via AFM and MS

The surface of the NRs was sensitized by means of covalent immobilization of aptamers against the target CA 125 protein, as described in Section 2.5. Individual NRs were sensitized via the precise dispensing of nanoliter microdrops of solution of the aptamers onto their surface. Figure 2 shows that the microdrops did not merge, thus confirming the formation of individual sensor areas, with different aptamers immobilized in each area.

The efficiency of the sensitization technique employed was confirmed via AFM and MS, with the use of SOI wafers as AFM substrates, as described in Section 2. Figure 3a displays a typical AFM image of the SOI substrate surface obtained after its sensitization with aptamers against CA 125.

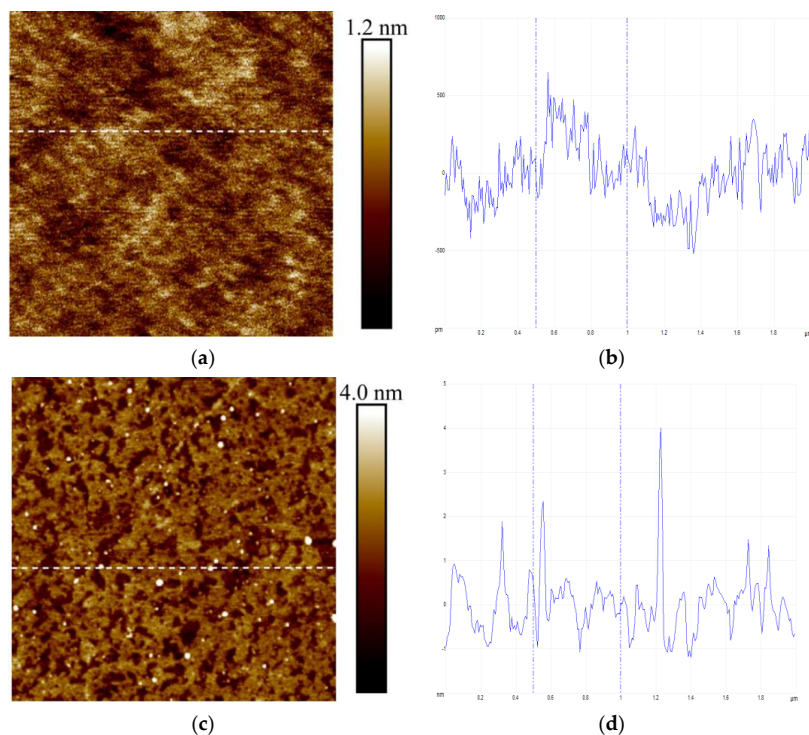


Figure 3. Typical AFM images of the SOI substrate surface (a,c) and cross-section profiles corresponding to the thick dashed lines in the AFM images (b,d), obtained after the silanization of the substrate surface (a), and after the incubation of the substrate in 10-nM solution of CA 125 (b). Scan size: $2 \times 2 \mu\text{m}^2$; Z scale: from 0 to 1.2 nm (a), from 0 to 4.0 nm (b).

The AFM image in Figure 3a indicates that the roughness of the APTES-silanized SOI substrate surface did not exceed 1.2 nm. At that, the number of objects with height greater than 1.0 nm amounted to ~200 per 400 μm^2 area. The latter did not exceed the noise value characteristic of highly sensitive AFM-based protein detection, which makes up 500 objects per 400 μm^2 [44].

A typical AFM image of the aptamer-sensitized SOI substrate surface, obtained after its incubation in the 10-nM CA 125 solution, is shown in Figure 3b. This AFM image indicates that objects with heights of up to 4 nm were visualized on the substrate surface with immobilized aptamers after its incubation in the CA 125 solution. These objects have been attributed to aptamer–antigen complexes, since complexes of gp120 (whose molecular weight is 110 kDa, i.e., close to that of CA 125) with immobilized aptamers were demonstrated to have similar heights [39].

After that, mass spectrometry analysis (MS analysis) was carried out in order to identify the molecules captured onto the surface of the SOI substrates. Figure 4 displays typical MALDI mass spectra of objects captured onto the SOI substrate surface after its incubation in 10-nM CA 125 solution. As a result of analysis of the mass spectra obtained, 60 peaks and 42 peaks, attributed to CA 125, were identified on SOI substrates No. 1 and No. 2, respectively (see Figure 4); furthermore, 3 peaks were attributed to the trypsin autolysis, and 14 peaks were attributed to keratin 1 of the human epidermis (AC UniProt P08779 and P13645, respectively). Thus, the MS analysis confirmed the efficiency of the SOI surface sensitization technique developed.

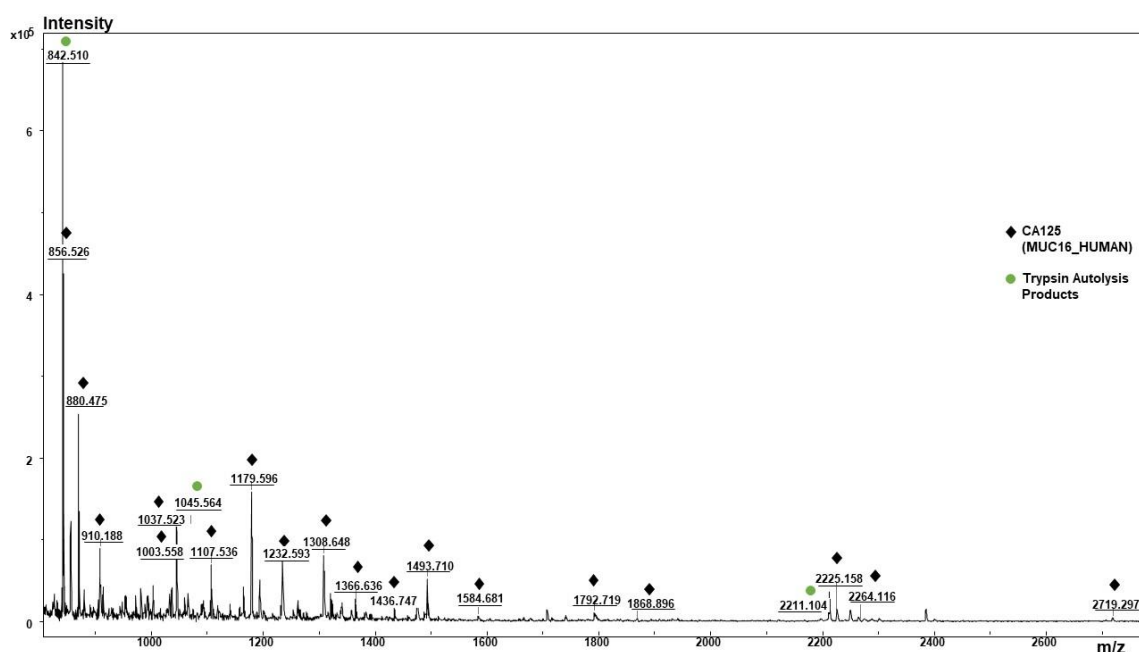


Figure 4. MALDI mass spectra of objects captured onto the surface of SOI substrate No. 1 after its incubation in 10-nM solution of CA 125. Markers indicate CA 125-related peptides (rhombs) and trypsin autolysis peaks (circles).

3.2. Detection of CA 125 in Potassium Phosphate Buffer

Figure 5a displays typical sensograms recorded before and after the addition of CA 125 solutions to the measuring cell. The curves shown in Figure 5a indicate an increase in the signal from the NRs with immobilized aptamers after the addition of CA 125 solutions. This increase in the biosensor signal occurs at the expense of a biospecific interaction between the target CA 125 molecules with the nanoribbon-immobilized aptamer probes. Moreover, a decrease in the biosensor signal with the decrease in the target protein concentration from 1 fM to 10 aM was also observed. As can be seen from the curves presented, the target

protein was detectable even at 22-aM concentration. Furthermore, substituting the CA 125 solution in the cell with a fresh, protein-free buffer induced a dissociation of the complexes formed by nanoribbon-immobilized aptamers and the target protein, thus leading to a decrease in the biosensor signal level. Accordingly, repeated use of the aptamer-sensitized nanoribbon sensor chips for the detection of CA 125 is possible.

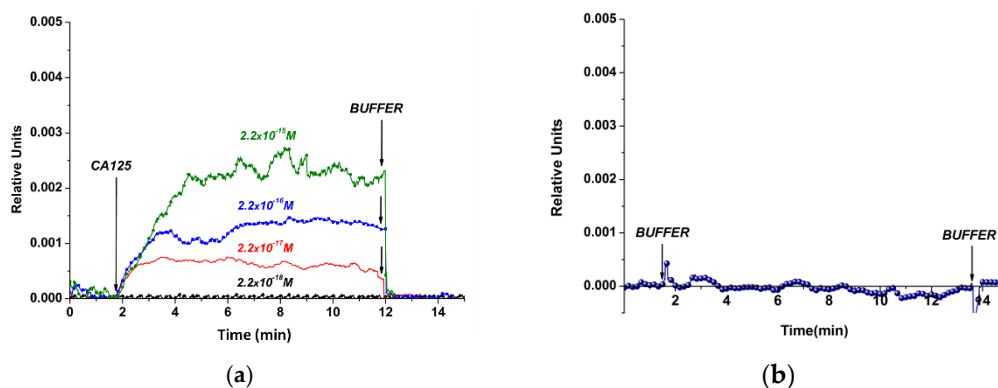


Figure 5. Typical sensogram curves obtained upon the detection of CA 125 protein in buffer solution at various concentrations of the target protein, using n-type nanoribbon sensor chips with covalently immobilized aptamers (a). Typical sensogram curve, obtained upon the analysis of protein-free solution (b). Experimental conditions: 1-mM potassium phosphate (KP) buffer, pH 7.4, $V_g = +50$ V; $V_{ds} = 0.2$ V. The total volume of the solution in the cell was 450 μ L. Arrows indicate addition of the CA 125 solution (with concentrations from 2 aM to 2 fM, as indicated in (a)) and washing with pure protein-free KP buffer.

The blank experiments were performed in order to find out whether there is an influence on the biosensor signal from the addition of pure buffer solution. Figure 5b displays a typical curve obtained upon the addition of pure protein-free 1-mM potassium phosphate working buffer instead of CA 125 solution. This curve clearly indicates the absence of any significant change in the biosensor signal in this case. The biosensor response signal, registered in the blank experiments, was no greater than 2% of the baseline signal level. The results obtained indicate a biospecific interaction between the nanoribbon-immobilized aptamer probes and the target CA 125 protein molecules, which were captured from the analyzed solutions onto the sensor surface.

Figure 6 displays the dependence of the level of the biosensor signal on the concentration of the target CA 125 protein. This dependence was plotted based on all of the data obtained in all of our experiments on the detection of CA 125 in buffer solution.

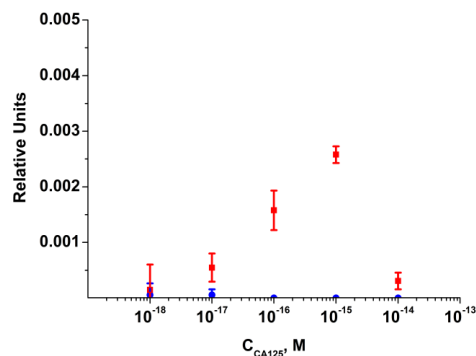


Figure 6. Dependence of the level of the biosensor signal on the concentration of CA 125 in buffer, obtained using nanoribbons of n-type conductance, sensitized with covalently immobilized aptamers. The number of technical replicates was $n = 3$. Circles (●) and squares (■) indicate the average value of the signal level before and after the addition of the CA 125 solution, respectively.

The dependence shown in Figure 6 indicates that at 22 fM and higher concentrations of the target protein, no difference between the signals from the control NRs and working NRs was observed. This can occur due to a high degree of non-specific binding of the target protein to the control NR surface. A large number of surface-bound molecules can cause aggregation of the target protein on the surface, thus leading to a change in the physicochemical characteristics of the (target protein)–(sensor surface) interaction. For instance, the efficiency of the protein adsorption onto the surface of the control NR can alter.

3.3. Detection of CA 125 in Plasma Samples

These experiments were performed in order to determine whether our NR biosensor is applicable for the detection of CA 125 in plasma samples obtained from ovarian cancer patients. Plasma from a healthy volunteer was used as a control sample. Figure 7 displays typical sensograms obtained upon the detection of CA 125 in these plasma samples.

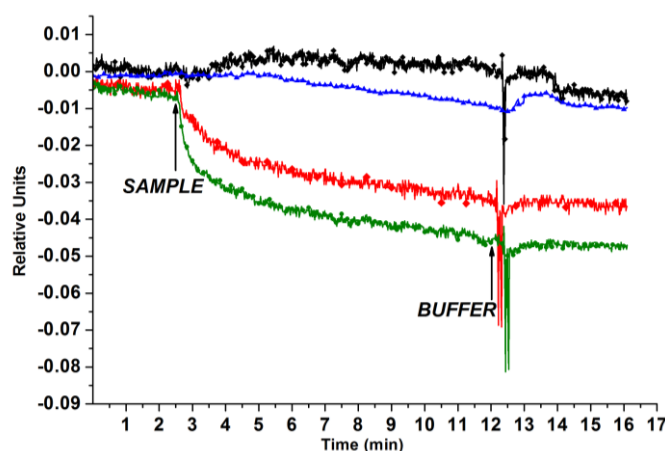


Figure 7. Results obtained upon the analysis of 10 plasma samples for the presence of CA 125 with the NR biosensor. The plasma samples were obtained from healthy volunteers (control samples; black and blue curves) and from ovarian cancer patients (sample # 60, red curve; sample #67, green curve). Experimental conditions: 1-mM potassium phosphate (KP) buffer, pH 7.4; $V_g = +50$ V; $V_{ds} = 0.2$ V. The total volume of the solution in the cell was 107 μ L. Arrows indicate the addition of the analyzed plasma samples and washing with pure protein-free KP buffer.

The curves displayed in Figure 7 indicate a significant change in the level of the NR biosensor signal after the addition of the sample of ovarian cancer patients (red and green curves). This is in contrast to the case of the control samples of healthy volunteers (black and blue curves), where virtually no change in the biosensor signal was registered. It is interesting to note that the level of the signal obtained upon the analysis of sample #67 (serous papillary adenocarcinoma, TNM stage T3cNXM1)—of a patient with a more serious tumor stage—is considerably higher than that in the case of sample #60 (serous moderate ovarian tumor, TNM stage T1ANXM0). This indicates that the more serious the tumor stage is, the higher is the level of the biosensor signal.

4. Discussion

The results obtained in our study indicate that nanoribbon-immobilized aptamers retain their affinity, thus allowing for the biospecific capture of the target CA 125 protein onto the nanoribbon surface. Once again, important advantages of using aptamers in biosensors include their small size [42], high time stability, and high chemical resistance [27,28]. These advantages have allowed us to attain a concentration limit of CA 125 detection an order of magnitude lower—in comparison with that attained with using antibodies as nanoribbon-immobilized molecular probes [12]. In our experiments reported herein, the lowest detectable concentration of the target CA 125 protein amounted to 22 aM (which is

equal to 0.033 pg/mL), while in the case of the antibody-functionalized sensor chips this concentration was as high as 150 fM [12].

In biosensors intended for the biospecific detection of target molecules, the sensor surface is sensitized with molecular probes against the target molecules. For instance, antibodies are widely employed for the detection of antigens [5–8,12]. It should be emphasized that upon dispensing the nanoliter drops of solution of molecular probes onto the nanoribbon sensor chip surface during the sensitization of individual nanoribbons (see Section 2.5), the area of the resulting spot is considerably larger than that of the nanoribbon itself. Due to this fact, the number of target molecules that are biospecifically captured directly onto the nanoribbon surface at femtomolar concentrations can be small, and their detection can thus be difficult. Nevertheless, in a number of papers, successful detection of biological molecules at such low concentrations is reported, thus indicating that it is relatively easy to attain such a low detection limit with a nanoribbon biosensor. We assume that this phenomenon is explained by a cooperative effect, which is caused by the formation of a network of bonds through a hydration shell within the near-surface layer. This network apparently participates in the transfer of charge from the point of complex formation to the nanoribbon surface.

The difference between the signals obtained for the samples of ovarian cancer patients and those obtained for the samples of healthy volunteers indicates the applicability of our biosensor for the detection of CA 125 in plasma. Thus, the NR biosensor allows one to perform label-free detection of target protein molecules in real time, without their additional amplification. In the future, the approach proposed herein can be used in clinical practice for the diagnosis of oncological pathologies in humans.

5. Conclusions

Herein, the highly sensitive detection of a cancer-associated protein marker—carbohydrate antigen CA 125—was performed in a buffer solution at pH 7.4 with the use of a nanoribbon (NR) biosensor. Sensor chips, based on “silicon-on-insulator” (SOI) structures of n-type conductance, fabricated using top-down CMOS-compatible technology, were employed. The surface of the NR sensors was sensitized with aptamers against the target protein. Via AFM, successful formation of 4-nm-high aptamer–antigen complexes was revealed on the surface of SOI substrates with immobilized aptamers against CA 125 after their incubation in 10-nM CA 125 solution. Protein components of macromolecular complexes were subsequently identified via MALDI-TOF-MS. Almost all of the identified peaks relate to the target CA 125 protein. These results confirm the sufficient efficiency of the aptamer immobilization technique employed for the SOI NR sensitization. The use of aptamer-sensitized NR sensor chips allowed us to experimentally attain the concentration limit of CA 125 detection at the level of 10 aM, which is an order of magnitude lower than that in the case of using anti-CA 125 antibodies as nanoribbon-immobilized molecular probes. The results reported indicate that the NR biosensor represents a promising tool for the revelation of ovarian cancer. Moreover, since in our NR biosensor a sensor chip bearing an array of 12 nanoribbons is utilized, its application will allow one to perform multiplexed detection of a number of biomarkers in a single sample.

Author Contributions: Conceptualization, Y.D.I., V.P.P. and A.I.A.; methodology, T.O.P.; software, R.A.G. and V.S.Z.; validation, T.O.P., A.I.I. and O.F.P.; formal analysis, V.Y.T. and A.V.G.; investigation, K.A.M., A.F.K., R.A.G., I.D.S., I.A.I., S.I.K., A.I.I., F.V.T. and V.S.Z.; resources, V.P.P., F.V.T., O.F.P., N.E.K., A.A.A. and A.V.G.; visualization, K.A.M., I.D.S., I.A.I. and A.I.I.; data curation, K.A.M., S.I.K., I.A.I., A.I.I. and A.F.K.; writing—original draft preparation, K.A.M., T.O.P. and I.D.S.; writing—review and editing, Y.D.I.; project administration, Y.D.I.; funding acquisition, A.I.A.; supervision, A.I.A. All authors have read and agreed to the published version of the manuscript.

Funding: This work was financed by the Ministry of Science and Higher Education of the Russian Federation within the framework of state support for the creation and development of World-Class Research Centers “Digital biodesign and personalized healthcare” No. 075-15-2020-913.

Institutional Review Board Statement: The study was conducted in accordance with the guidelines of the Declaration of Helsinki and in compliance with Order no. 1177n (the Ministry of Health of the Russian Federation, 20 December 2012), and approved by the independent Local Ethical Committee of N.N. Blokhin National Medical Research Center of Oncology, the Ministry of Health of the Russian Federation (Protocol approval date: 28 November 2019).

Informed Consent Statement: Informed consent was obtained from all subjects involved in the study.

Data Availability Statement: The data obtained throughout the experiments can be provided by Yu.D.I. upon reasonable request.

Acknowledgments: The biosensor measurements were performed employing a nanoribbon detector, which pertains to “Avogadro” large-scale research facilities. The AFM measurements were performed employing a Dimension FastScan Bio multimode atomic force microscope, which pertains to “Avogadro” large-scale research facilities.

Conflicts of Interest: The authors declare no conflict of interest.

References

1. Rissin, D.M.; Kan, C.W.; Campbell, T.G.; Howes, S.C.; Fournier, D.R.; Song, L.; Piech, T.; Patel, P.P.; Chang, L.; Rivnak, A.J.; et al. Single-Molecule Enzyme-Linked Immunosorbent Assay Detects Serum Proteins at Subfemtomolar Concentrations. *Nat. Biotechnol.* **2010**, *28*, 595–599. [\[CrossRef\]](#)
2. Johari-Ahar, M.; Rashidi, M.R.; Barar, J.; Aghaie, M.; Mohammadnejad, D.; Ramazani, A.; Karami, P.; Coukos, G.; Omid, Y. An ultra-sensitive impedimetric immunosensor for detection of the serum oncomarker CA-125 in ovarian cancer patients. *Nanoscale* **2015**, *7*, 3768–3779. [\[CrossRef\]](#)
3. Archakov, A.I.; Ivanov, Y.D.; Lisitsa, A.V.; Zgoda, V.G. AFM fishing nanotechnology is the way to reverse the Avogadro number in proteomics. *Proteomics* **2007**, *7*, 4–9. [\[CrossRef\]](#) [\[PubMed\]](#)
4. Fägerstam, L.G. Biospecific Interaction Analysis in Real Time Using a Biosensor System with Surface Plasmon Resonance Detection. In *Applied Virology Research*; Kurstak, E., Marusyk, R.G., Murphy, F.A., Van Regenmortel, M.H.V., Eds.; Springer: Boston, MA, USA, 1994; Volume 3. [\[CrossRef\]](#)
5. Stern, E.; Vacic, A.; Rajan, N.K.; Criscione, J.M.; Park, J.; Ilic, B.R.; Mooney, D.J.; Reed, M.A.; Fahmy, T.M. Label-free biomarker detection from whole blood. *Nat. Nanotechnol.* **2010**, *5*, 138–142. [\[CrossRef\]](#)
6. Patolsky, F.; Zheng, G.F.; Hayden, O.; Lakadamyali, M.; Zhuang, X.; Lieber, C.M. Electrical detection of single viruses. *Proc. Natl. Acad. Sci. USA* **2004**, *101*, 14017–14022. [\[CrossRef\]](#) [\[PubMed\]](#)
7. Zheng, G.; Patolsky, F.; Cui, Y.; Wang, W.U.; Lieber, C.M. Multiplexed electrical detection of cancer markers with nanowire sensor arrays. *Nat. Biotechnol.* **2005**, *23*, 1294–1301. [\[CrossRef\]](#)
8. Ivanov, Y.; Pleshakova, T.; Kozlov, A.; Malsagova, K.; Krohin, N.; Shumyantseva, V.; Shumov, I.; Popov, V.; Naumova, O.; Fomin, B.; et al. SOI nanowire for the high-sensitive detection of HBsAg and α -fetoprotein. *Lab Chip* **2012**, *12*, 5104–5111. [\[CrossRef\]](#) [\[PubMed\]](#)
9. Malsagova, K.; Ivanov, Y.; Pleshakova, T.; Kaysheva, A.; Shumov, I.; Kozlov, A.; Archakov, A.; Popov, V.; Fomin, B.; Latyshev, A. A SOI-nanowire biosensor for the multiple detection of D-NFATc1 protein in the serum. *Anal. Methods* **2015**, *7*, 8078–8085. [\[CrossRef\]](#)
10. Ivanov, Y.; Pleshakova, T.; Kozlov, A.; Malsagova, K.; Krohin, N.; Kaysheva, A.; Shumov, I.; Archakov, A.; Popov, V.; Naumova, O.; et al. SOI nanowire transistor for detection of D-NFATc1 molecules. *Optoelectron. Instrum. Data Process.* **2013**, *49*, 520–525. [\[CrossRef\]](#)
11. Malsagova, K.A.; Pleshakova, T.O.; Galiullin, R.A.; Kaysheva, A.L.; Shumov, I.D.; Ilnitskii, M.A.; Popov, V.P.; Glukhov, A.V.; Archakov, A.I.; Ivanov, Y.D. Ultrasensitive nanowire-based detection of HCVcoreAg in the serum using a microwave generator. *Anal. Methods* **2018**, *10*, 2740–2749. [\[CrossRef\]](#)
12. Malsagova, K.A.; Pleshakova, T.O.; Galiullin, R.A.; Kozlov, A.F.; Shumov, I.D.; Popov, V.P.; Tikhonenko, F.V.; Glukhov, A.V.; Ziborov, V.S.; Petrov, O.F.; et al. Highly Sensitive Detection of CA 125 Protein with the Use of an n-Type Nanowire Biosensor. *Biosensors* **2020**, *10*, 210. [\[CrossRef\]](#)
13. Malsagova, K.A.; Pleshakova, T.O.; Galiullin, R.A.; Shumov, I.D.; Kozlov, A.F.; Romanova, T.S.; Popov, V.P.; Glukhov, A.V.; Konev, V.A.; Archakov, A.I.; et al. Nanowire Aptamer-Sensitized Biosensor Chips with Gas Plasma-Treated Surface for the Detection of Hepatitis C Virus Core Antigen. *Coatings* **2020**, *10*, 753. [\[CrossRef\]](#)
14. Hahm, J.; Lieber, C.M. Direct ultrasensitive electrical detection of DNA and DNA sequence variations using nanowire nanosensors. *Nano Lett.* **2004**, *4*, 51–54. [\[CrossRef\]](#)
15. Lin, C.-H.; Hung, C.-H.; Hsiao, C.-Y.; Lin, H.-C.; Ko, F.-H.; Yang, Y.-S. Poly-silicon nanowire field-effect transistor and label-free detection of pathogenic avian influenza DNA. *Biosens. Bioelectron.* **2009**, *24*, 3019–3024. [\[CrossRef\]](#)
16. Ivanov, Y.; Pleshakova, T.; Malsagova, K.; Kozlov, A.; Kaysheva, A.; Shumov, I.; Galiullin, R.; Kurbatov, L.; Popov, V.; Naumova, O.; et al. Detection of marker miRNAs in plasma using SOI-NW biosensor. *Sens. Actuat. B Chem.* **2018**, *261*, 566–571. [\[CrossRef\]](#)

17. Malsagova, K.A.; Pleshakova, T.O.; Galiullin, R.A.; Kozlov, A.F.; Romanova, T.S.; Shumov, I.D.; Popov, V.P.; Tikhonenko, F.V.; Glukhov, A.V.; Smirnov, A.Y.; et al. SOI-Nanowire Biosensor for the Detection of Glioma-Associated miRNAs in Plasma. *Chemosensors* **2020**, *8*, 95. [CrossRef]
18. Malsagova, K.A.; Pleshakova, T.O.; Kozlov, A.F.; Shumov, I.D.; Ilnitskii, M.A.; Miakonkikh, A.V.; Popov, V.P.; Rudenko, K.V.; Glukhov, A.V.; Kupriyanov, I.N.; et al. Micro-Raman Spectroscopy for Monitoring of Deposition Quality of High-k Stack Protective Layer onto Nanowire FET Chips for Highly Sensitive miRNA Detection. *Biosensors* **2018**, *8*, 72. [CrossRef] [PubMed]
19. Ivanov, Y.; Pleshakova, T.; Malsagova, K.; Kurbatov, L.; Popov, V.; Glukhov, A.; Smirnov, A.; Enikeev, D.; Potoldykova, N.; Alekseev, B.; et al. Detection of Marker miRNAs, Associated with Prostate Cancer, in Plasma Using SOI-NW Biosensor in Direct and Inversion Modes. *Sensors* **2019**, *19*, 5248. [CrossRef] [PubMed]
20. Tian, R.; Regonda, S.J.; Gao, J.; Liu, Y.; Hu, W. Ultrasensitive protein detection using lithographically defined Si multi-nanowire field effect transistors. *Lab Chip* **2011**, *11*, 19552–19561. [CrossRef]
21. Patolsky, F.; Zheng, G.; Lieber, C.M. Fabrication of silicon nanowire devices for ultrasensitive, label-free, real-time detection of biological and chemical species. *Nat. Protoc.* **2006**, *1*, 1711–1724. [CrossRef]
22. Elfström, N.; Juhasz, R.; Sychugov, I.; Engfeldt, T.; Karlström, A.E.; Linnros, J. Surface charge sensitivity of silicon nanowires: Size dependence. *Nano Lett.* **2007**, *7*, 2608–2612. [CrossRef]
23. Wenga, G.; Jacques, E.; Salaün, A.-C.; Rogel, R.; Pichon, L.; Geneste, F. Bottom-gate and step-gate polysilicon nanowires field effect transistors for ultrasensitive label-free biosensing application. *Procedia Eng.* **2012**, *47*, 414–417. [CrossRef]
24. Ivanov, Y.D.; Pleshakova, T.O.; Popov, V.P.; Naumova, O.V.; Aseev, A.L.; Archakov, A.I. SOI-Nanowire Biosensors for High-Sensitivity Protein and Gene Detection. In *Functional Nanomaterials and Devices for Electronics, Sensors and Energy Harvesting*; Nazarov, A., Balestra, F., Kilchytska, V., Flandre, D., Eds.; Springer: Cham, Switzerland; London, UK, 2014; pp. 445–467. [CrossRef]
25. Huang, J.; Lin, Q.; Yu, J.; Ge, S.; Li, J.; Yu, M.; Zhao, Z.; Wang, X.; Zhang, X.; He, X.; et al. Comparison of a Resonant Mirror Biosensor (IASys) and a Quartz Crystal Microbalance (QCM) for the Study on Interaction between *Paeoniae Radix* 801 and Endothelin-1. *Sensors* **2008**, *8*, 8275–8290. [CrossRef] [PubMed]
26. Zhang, G.-J.; Chai, K.T.C.; Luo, H.Z.H.; Huang, J.M.; Tay, I.G.K.; Lim, A.; Eu, -J.; Je, M. Multiplexed detection of cardiac biomarkers in serum with nanowire arrays using readout ASIC. *Biosens. Bioelectron.* **2012**, *35*, 218–223. [CrossRef] [PubMed]
27. Arshavsky-Graham, S.; Urmann, K.; Salam, R.; Massad-Ivanir, N.; Walter, J.-G.; Scheper, T.; Segal, E. Aptamers vs. antibodies as capture probes in optical porous silicon biosensors. *Analyst* **2020**, *145*, 4991–5003. [CrossRef]
28. Lee, J.-O.; So, H.-M.; Jeon, E.-K.; Chang, H.; Won, K.; Kim, Y.H. Aptamers as molecular recognition elements for electrical nanobiosensors. *Anal. Bioanal. Chem.* **2008**, *390*, 1023–1032. [CrossRef]
29. Available online: <https://www.cancer.org/cancer/ovarian-cancer/about/key-statistics.html> (accessed on 29 January 2021).
30. Office for National Statistics, Cancer Survival by Stage at Diagnosis for England. 2019. Available online: <https://www.ons.gov.uk/peoplepopulationandcommunity/healthandsocialcare/conditionsanddiseases/datasets/cancersurvivalratescancersurvivalinenglandadultsdiagnosed> (accessed on 29 January 2021).
31. Kushlinskii, N.E.; Krasil'nikov, M.A. *Biological Tumor Markers: Basic and Clinical Research*; RAMS Publishing House: Moscow, Russia, 2017.
32. Bast, R.C., Jr. Status of tumor markers in ovarian cancer screening. *J. Clin. Oncol.* **2003**, *21* (Suppl. S10), 200s–205s. [CrossRef]
33. Szymańska, B.; Lukaszewski, Z.; Hermanowicz-Szamatowicz, K.; Gorodkiewicz, E. A biosensor for determination of the circulating biomarker CA 125/MUC16 by Surface Plasmon Resonance Imaging. *Talanta* **2019**, *206*, 120187. [CrossRef] [PubMed]
34. Mandal, D.; Nunna, B.B.; Zhuang, S.; Rakshit, S.; Lee, E.S. Carbon nanotubes based biosensor for detection of cancer antigens (CA-125) under shear flow condition. *Nano Struct. Nano Objects* **2018**, *15*, 180–185. [CrossRef]
35. Attia, M.S.; Ali, K.; El-Kemari, M.; Darwish, W.M. Phthalocyanine-doped polystyrene fluorescent nanocomposite as a highly selective biosensor for quantitative determination of cancer antigen 125. *Talanta* **2019**, *201*, 185–193. [CrossRef]
36. Petrova, I.; Konopsky, V.; Nabiev, I.; Sukhanova, A. Label-Free Flow Multiplex Biosensing via Photonic Crystal Surface Mode Detection. *Sci. Rep.* **2019**, *9*, 8745. [CrossRef] [PubMed]
37. Naumova, O.V.; Fomin, B.I.; Nasimov, D.A.; Dudchenko, N.V.; Devyatova, S.F.; Zhanaev, E.D.; Popov, V.P.; Latyshev, A.V.; Aseev, A.L.; Ivanov, Y.D.; et al. SOI Nanowires as Sensors for Charge Detection. *Semicond. Sci. Technol.* **2010**, *25*, 055004. [CrossRef]
38. Ivanov, Y.D.; Kaysheva, A.L.; Frantsuzov, P.A.; Pleshakova, T.O.; Krohin, N.V.; Izotov, A.A.; Shumov, I.D.; Uchaikin, V.F.; Konev, V.A.; Ziborov, V.S.; et al. Detection of hepatitis C virus core protein in serum by atomic force microscopy combined with mass spectrometry. *Int. J. Nanomed.* **2015**, *10*, 1597–1608. [CrossRef]
39. Ivanov, Y.D.; Bukharina, N.S.; Pleshakova, T.O.; Frantsuzov, P.A.; Andreeva, E.Y.; Kaysheva, A.L.; Zgoda, V.G.; Izotov, A.A.; Pavlova, T.I.; Ziborov, V.S.; et al. Atomic force microscopy fishing and mass spectrometry identification of gp120 on immobilized aptamers. *Int. J. Nanomed.* **2014**, *9*, 4659–4670. [CrossRef]
40. Pleshakova, T.O.; Kaysheva, A.L.; Shumov, I.D.; Ziborov, V.S.; Bayzhanova, J.M.; Konev, V.A.; Uchaikin, V.F.; Archakov, A.I.; Ivanov, Y.D. Detection of Hepatitis C Virus Core Protein in Serum Using Aptamer-Functionalized AFM Chips. *Micromachines* **2019**, *10*, 129. [CrossRef] [PubMed]
41. Kaysheva, A.L.; Pleshakova, T.O.; Stepanov, A.A.; Ziborov, V.S.; Saravanabhavan, S.S.; Natesan, B.; Archakov, A.I.; Ivanov, Y.D. Immuno-MALDI MS dataset for improved detection of HCVcoreAg in sera. *Data Brief.* **2019**, *25*, 104240. [CrossRef] [PubMed]

42. Pleshakova, T.O.; Kaysheva, A.L.; Bayzyanova, J.M.; Anashkina, A.S.; Uchaikin, V.F.; Shumov, I.D.; Ziborov, V.S.; Konev, V.A.; Archakov, A.I.; Ivanov, Y.D. Advantages of aptamers as ligands upon protein detection by AFM-based fishing. *Anal. Meth.* **2017**, *9*, 6049–6060. [[CrossRef](#)]
43. Ivanov, Y.D.; Pleshakova, T.O.; Krohin, N.V.; Kaysheva, A.L.; Usanov, S.A.; Archakov, A.I. Registration of the protein with compact disk. *Biosens. Bioelectron.* **2013**, *43*, 384–390. [[CrossRef](#)]
44. Ivanov, Y.D.; Danichev, V.V.; Pleshakova, T.O.; Shumov, I.D.; Ziborov, V.S.; Krokhin, N.V.; Zagumenniy, M.N.; Ustinov, V.S.; Smirnov, L.P.; Shironin, A.V.; et al. Irreversible chemical AFM-based fishing for detection of low-copied proteins. *Biochem. (Moscow) Suppl. Ser. B Biomed. Chem.* **2013**, *7*, 46–61. [[CrossRef](#)]